3

Wind Tunnels for the Study of Particle Transport

Keld Rømer Rasmussen[1], Jonathan Peter Merrison[2] and Per Nørnberg[1]
[1]*Aarhus University, Department of Goscience,*
[2]*Aarhus University, Department of Physics and Astronomy*
Denmark

1. Introduction

Wind tunnels for investigating the effect of wind on sand and soil movement have been constructed by many groups since Brigadier R.A. Bagnold build one of the first wind tunnels for investigating the threshold of motion of sand (Bagnold 1941). Initiated by the serious soil erosion in the American Midwest during the 1930's another wind tunnel facility was set up later in the decade at Kansas State University at the USDA-ARS Wind Erosion Research Unit for soil erosion research. A wind tunnel for studying particle motion under fluid densities as on the planet Mars was as the first of its kind build at the NASA Ames Research Centre, California in the mid 1970's under guidance of Dr. Ronald Greeley (Greeley et al. 1981). The wind tunnel laboratory at Aarhus University was started in the 1970's and have to day two sand transport wind tunnels and two low pressure wind tunnels for studying sand and dust transport under Martian conditions. This chapter will deal with descriptions of the materials used in wind tunnel experiments and research lay-outs for the wind tunnels at the Aarhus University wind tunnel laboratory.

2. Sand and dust size materials in wind tunnel experiments

2.1 Particle size classification

Over time a number of slightly different scales have been used in dividing of loose sediments or soils in particle size fractions (Krumbein and Pettijohn 1938, Pettijohn 1957, Scheffer & Schachtschabel 1998). In European context the logarithmic φ-scale which is the same as 2^n or $\sqrt{2}^n$ are widely used and refer to sieve openings in millimetres. Here the limit between gravel and sand is set to 2mm, the limit between sand and silt to 0.063 mm and the limit between silt and clay to 0.002 mm. In USA these limits are slightly different and set up by the US Bureau of Soils. In this scale the gravel/sand limit is also 2 mm. The sand/silt limit 0.050 mm and the silt/clay limit 0.002 mm (Klute 1986, Ulery & Drees 2008).
In the field of Aeolian transport there are clear physical definitions for the descriptive terms of dust and sand. Dust grains are referred to as those which can be suspended by the atmosphere (i.e. turbulence within the flow is comparable to that of the gravitational settling velocity). Sand grains refer to particulates which can be entrained from a surface by the wind flow, but cannot be suspended. They therefore perform saltation, with repeated entrainment events and ballistic return to the surface. These definitions are physically meaningful in a particular wind flow environment, however they vary depending on the

properties of the particulates and the flow conditions and generally do not correspond to well-defined size categories. On Earth, in a typical natural environment, dust grains are typically less than 10μm as they are on Mars.

2.2 Particle size concept

Particles used in wind tunnel experiments are normally single grain particles if they are of sand size. But will often aggregate during transport if they are of silt and clay size. If the particles were all spheres, no special difficulty would arise in defining and determining their size. The diameter would be a well defined parameter. However, natural particles are of irregular shape, and generally more irregular the smaller the particles are.

Measurements of the particle diameters are commonly made though the irregular shape causes difficulties. A particle could be regarded as a matchbox 50x35x15 mm or a triaxial ellipsoid and it is obvious that the 3-dimensional form is not easily described by one unique number. The term diameter varies widely in meaning with respect to the way in which it is measured. All methods of measurements end up with regarding the particles as spheres, or that the measurements made can be expressed as diameter of equivalent spheres. However, as sand, silt and clay particles from nature are not spheres the reported sizes are incorrect or inaccurate. In the laboratory we have different methods of measuring particle sizes.

Sieves are commonly used to separate and measure particles of loose single grain materials. But sieves do not measure size alone. Long cigar shaped particles may pass a sieve and be weighed with particles of a smaller volume but a more regular shape. Thus sieves classify particles on the basis of their smallest cross section. The holes in sieves have a certain size distribution and laboratory experiments show that the longer sieving times the bigger particles get through the sieves (pers. com. Dalsgaard, K.). They find the bigger holes.

Sedimentation after Stoke's law is another way of sorting particles. This is a classic statement of settling velocity of spherical particles. Under standard conditions, constant temperature, a given fluid, and a known specific gravity of the spheres $v = Cr^2$, where v is the velocity in cm pr. second, r is the radius of the sphere in cm, and C is a constant equal to $(2/9)\ (d_1 - d_2)\ g/\eta$. d_1 and d_2 are the densities of the sphere and the fluid, respectively, g is gravity acceleration, and η is the viscosity. Stokes law has been shown to hold for particles of silt size and smaller down to where Brownian movement influences the settling velocities. Sedimentation of the silt and clay size fractions for particle size determination is often done in sedimentation cylinders (Andreasen pipettes). However, if we look at particles collected in dunes of wind blown sand we can see that the equivalent diameter is a debatable expression. Figure 1, 2, 3 and 4 are from dune sand samples (Nørnberg 2002). An assumed density of 2.65 g/cm (quartz) is often used for natural particles, but talking about a nominal diameter as we do in Stokes law can be far away from realities, and when it comes to sedimentation in media that do not have a homogenous density like planet atmospheres this have to be taken into account.

In wind tunnel experiments glass spheres can be used to overcome problems with irregular particle shape. If we look at a single sand grain like Figure 5 it is obvious that there are a number of different answers to giving the size.

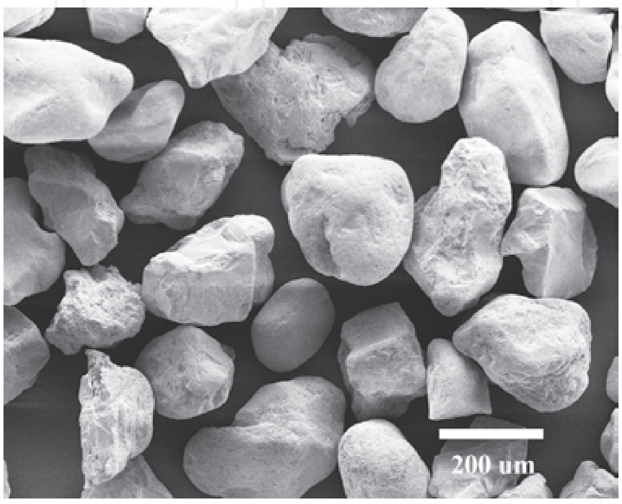

Fig. 1. Sand fraction 250-125 μm

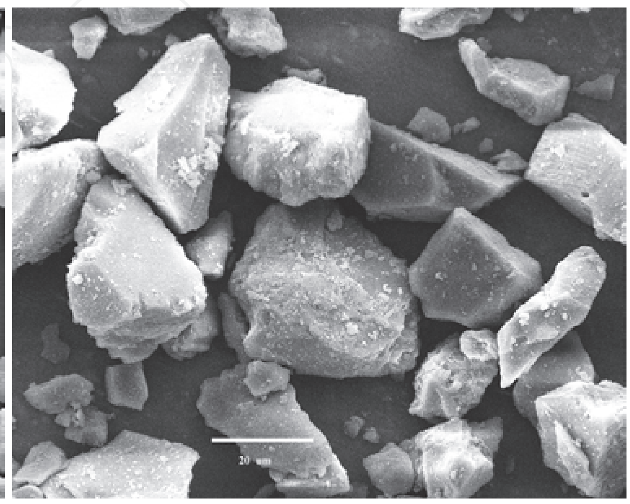

Fig. 2. Silt 63-20 μm

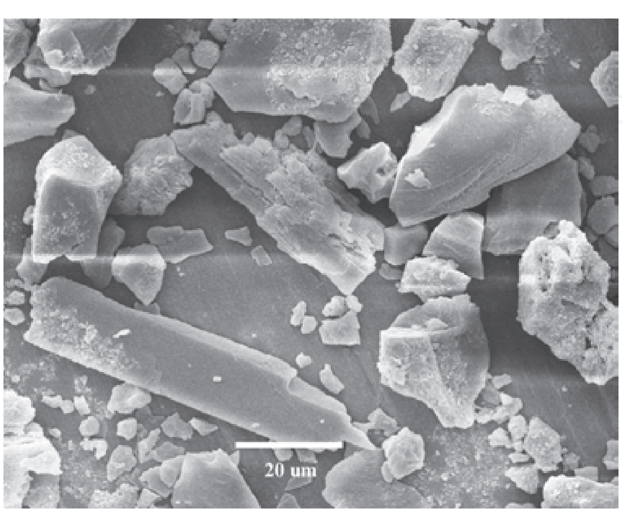

Fig. 3. Silt 20-2 μm

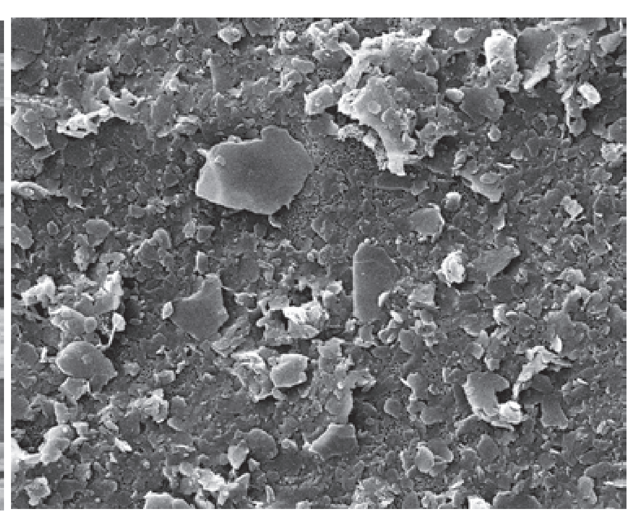

Fig. 4. Clay < 2 μm

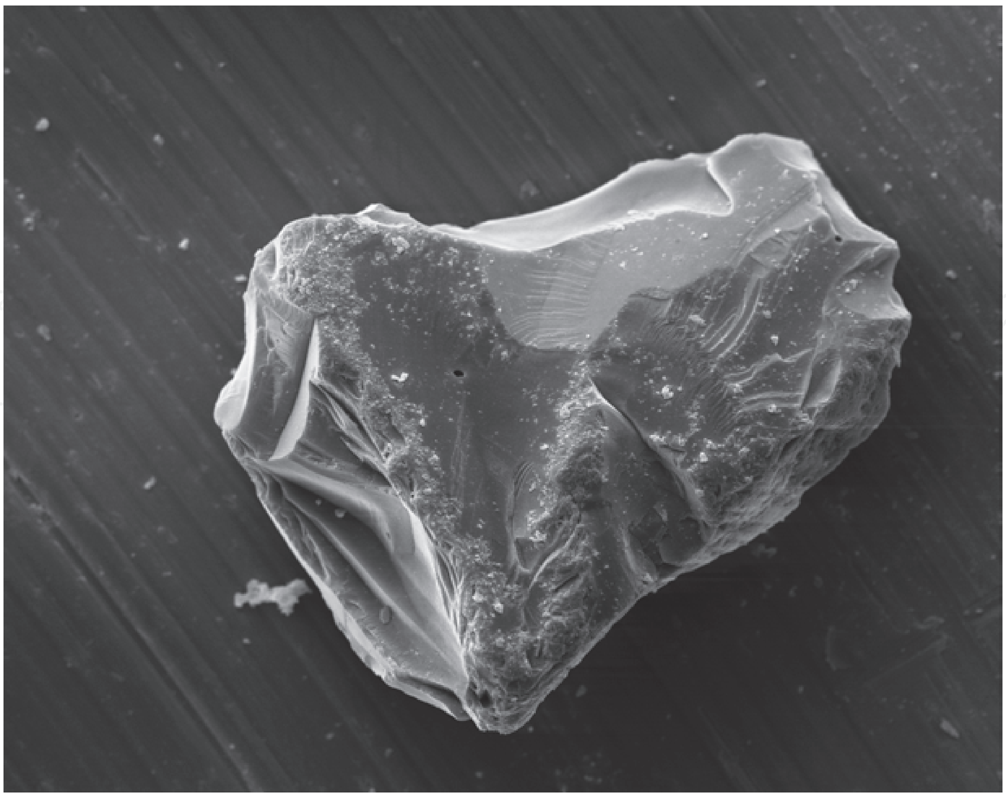

Fig. 5. A 100 μm sand grain.

It could be 1) a sphere of the same maximum length, 2) a sphere with the same minimum length, 3) a sphere with the same weight, 4) a sphere with the same sedimentation rate, 5) a sphere passing the same sieve aperture, 6) a sphere with the same surface area, or 7) a sphere with the same volume.

This also tells us that particle size standards for e.g. sand grains are defined by the technique used for the determination. Sieves are often used to split up sand fractions and sedimentation used for silt and clay size fractionation. This is however, two very different techniques if used for particle size distribution measurements, and it is often difficult to inter calibrate the two methods. An alternative method widely used in industry production and research laboratories is the laser diffraction method. This method is based on Low Angle Laser Light Scattering (LALLS).

A laser source of coherent light like a He-Ne gas laser with a wavelength of 633 nm is the most commonly used in laser diffraction (LD) instruments. A parallel beam of light is sent through a cuvette with suspended particles, either in water or air and a Fourier Transform Lens focuses the light scattered by the particles on a ring formed multi element detector. The advantage of using this method is that the whole particle range from < 2 μm to > 3.5 mm can be measured by the same technique. The laser diffraction system generates a volume distribution of the sample which is directly equal to the weight distribution if the density is constant. The volume is calculated to an equivalent sphere with a certain diameter. Data determined by LD is not directly comparable with sieving or pipette methods. However, the LD method based on volume is a valid, reproducible method that is very little time consuming (Eshel et al. 2004 and Beuselinck et al. 1998).

Examples on sand size materials used in the terrestrial wind tunnels, and silt size (dust) used in experiments in the low pressure Mars wind tunnels is seen in Table 1 (all LD determinations).

<table>
<tr><th>Sample</th><th>>500 µm</th><th>500-250 µm</th><th>250-125 µm</th><th>125-63 µm</th><th>63-32 µm</th><th>32-16 µm</th><th>16-8 µm</th><th>8-4 µm</th><th>4-2 µm</th><th><2 µm</th></tr>
<tr><td></td><td colspan="10">%</td></tr>
<tr><td>Sand (125µm)</td><td></td><td>1.52</td><td>80.36</td><td>15.24</td><td>0.78</td><td colspan="5">2.10</td></tr>
<tr><td>Sand (242µm)</td><td>0.99</td><td>74.49</td><td>22.96</td><td>1.08</td><td>0.40</td><td colspan="5">0.08</td></tr>
<tr><td>Glass balls 200-300 µm</td><td>2.77</td><td>64.53</td><td>31.16</td><td>1.42</td><td>0.08</td><td colspan="5">0.04</td></tr>
<tr><td>JSC-1</td><td></td><td>4.86</td><td>36.59</td><td>25.89</td><td>14.02</td><td>7.66</td><td>4.20</td><td>2.72</td><td>1.99</td><td>2.07</td></tr>
<tr><td>Salten Skov I < 63 µm</td><td></td><td></td><td>0.25</td><td>5.95</td><td>9.14</td><td>8.10</td><td>10.37</td><td>14.13</td><td>20.92</td><td>31.14</td></tr>
<tr><td>Clay (WB)</td><td></td><td></td><td>0.74</td><td>3.46</td><td>5.36</td><td>5.84</td><td>8.63</td><td>21.43</td><td>25.45</td><td>29.10</td></tr>
</table>

Table 1. Particle size data for wind tunnel materials

2.3 Mineralogy and chemistry of sand and dust

The sand material for experiments in the terrestrial wind tunnels is quartz sand from Miocene deposits. It contains traces of mica, but >99% of the sand is quartz. This material resembles dune sand in Denmark which has also very high quartz content.

The dust materials used in wind tunnel experiments under Mars conditions are chosen for mechanical physical properties reasons like particle size, magnetic properties, colour. These are properties which can be close to Mars dust conditions, while the chemistry is in most cases different from the chemical properties of the Martian dust. As seen in table 2 the chemical composition of JSC-1 described by Morris et al. (2001) and Moroz et al. (2009) and Salten Skov I (Nørnberg et al. 2004, Nørnberg et al. 2009) are very different, and as we have at present no quantitative chemical analyses of the dust on Mars the samples can not be compared with Mars samples. A number of other Mars analogue dust samples used World wide in experiments are described by Marlow et al. (2008). The magnetic properties of the atmospheric dust on Mars is estimated to have a saturation magnetization J_s of 2.5 Am^2/kg (Morris et al. 2001), which is not far from the J_s of dust captured by Morris at al. (2001) on the Mauna Kea volcano, Hawaii which was 2.5±1.5 Am^2/kg. This is significantly lower than J_s of the Salten Skov I, that is 3.9 (1) Am^2/kg (Nørnberg et al. 2009).

	SiO_2	TiO_2	Al_2O_3	Fe_2O_3	MnO	MgO	CaO	Na_2O	K_2O	P_2O_5	Vola-tiles	Sum
	---%---											
JSC-1	37.73	3.43	21.06	15.28	0.25	3.01	5.20	1.97	0.49	0.76	10.73	99.91
SS-1 < 63 μm	16.10	0.29	3.20	61.92	1.66	0.16	0.20	0.19	0.52	0.47	14.43	99.14

Table 2. Examples on chemical composition of silt size dust material

3. The one bar sand transport wind tunnels

3.1 The boundary layer wind tunnels

Before dealing with flow in aeolian wind tunnels it is expedient to introduce a few concepts and assumptions. Thus while the velocity field of flows in Nature is 3-dimensional (3-D) it is often simpler and described using a 2-D approximation in the wind tunnel. Thus for a wind tunnel with a rectangular test section, we may assume a 2-D flow having average horizontal velocity component u parallel to the tunnel (x-)axis and average velocity component w in the vertical (z-)direction. The corresponding fluctuating velocity components are u′ and w′. The boundary layer flow in the region immediately above the bed has shear stress τ defined as

$$\tau = -\rho\overline{u'w'} = \rho u_*^2$$

where u_* is the friction speed. The boundary layer has a logarithmic wind profile with u(z) given by

$$u(z) = \frac{u_*}{\kappa} ln \frac{z}{z_0}$$

with κ being the von Karmán's constant (0.4) and z_0 the aerodynamic roughness length. The friction speed at which grains can be dislodged from the bed under fluid force is the threshold friction speed (u_{*t}) while the equilibrium velocity of a particle settling through a fluid under gravity is the terminal speed (u_F). Both u_{*t} and u_F are functions of particle diameter (see e.g. Greeley and Iversen, 1987), and particle transport will take place if $u_* > u_{*t}$. Suspension will dominate for particles having $u_F < u_*$ while bedload (saltation or creep) will be the dominant transport mode if $u_F > u_*$ (Bagnold, 1941).

A boundary layer wind tunnel designed for testing the physics of the windborne transport of sand and dust is often referred to as an aeolian wind tunnel. Horizontal aeolian wind tunnels such as the primary wind tunnel at Aarhus University (figure 6) have been widely used to study in the laboratory processes related to sand drifting in the terrestrial as well as in planetary environments. A variety of issues have been studied such as the threshold for initiation of movement (Bagnold, 1941; Chepil, 1959; Iversen and Rasmussen, 1994), effects of grain impact and inter-particle forces (Iversen et al, 1976; Iversen et al, 1987) and the interaction between wind flow and sand transport rate (Bagnold, 1941; Williams, 1964; Owen, 1964; Rasmussen and Mikkelsen, 1991; Iversen and

Rasmussen, 1999). In nature, much sand transport (on sand dunes for example) takes place on sloping surfaces, but relatively few laboratory studies have been made in order to study the effects of slope. Therefore a second wind tunnel of variable slope was built at the Aarhus University (figure 7) and this has been used to investigate threshold and mass transport characteristics for sands of different grain sizes.

Both wind tunnels at Aarhus University are primarily made of wood. The horizontal aeolian wind tunnel (HW) is a 15 m long open circuit, suction type tunnel and the test section is 0.60 m wide and 0.90 m high. A small bell-mouth, with a screen attach to it, is placed at the inlet in order to reduce the effect from low frequency fluctuations distorting the natural turbulence characteristics of the internal boundary-layer. A sand feed mechanism follows one meter downwind of the inlet to maintain a constant transport rate downwind under the influence of a pre-designed boundary layer. Sand transported in the HW is trapped in a sand collector in the downwind end of the tunnel, just in front of the fan and motor. The working area is the section from 10-13 m downstream of the entry. The side panels of the tunnel body consists of a set of gates (windows) that can swing up thus permitting access to the interior. Another set of gates in the ceiling of the tunnel above the working section offer an alternative access to the working section. The latter set of gates is primarily used to install instruments which must be operated partly from the outside or connected to an external power supply or recording system.

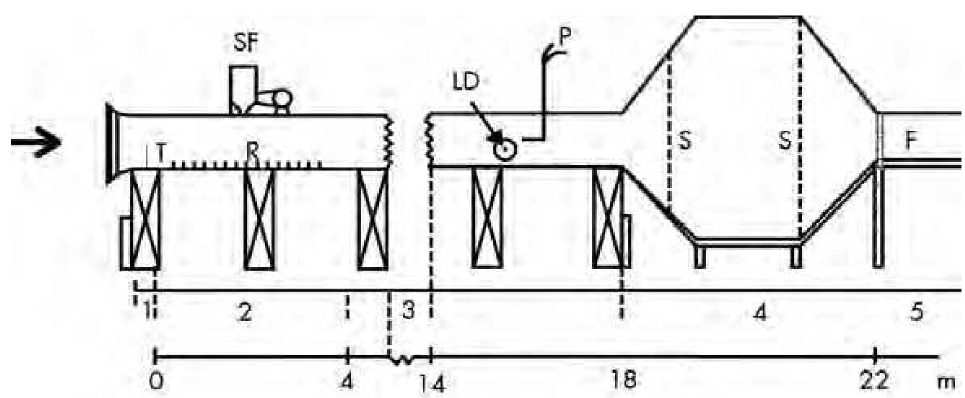

Fig. 6. The horizontal wind tunnel with main sections indicated: 1 – entry with screen (S) and bell mouth (B); 2 – boundary layer modification with turbulence spires (T), roughness array (R) and sand feed (F); 3 – working section with laser Doppler (LD) and Pitot-static tube (P); 4 – expansion box (sand collector) with screens (S); 5 – fan (F) and exhaust.

The variable slope wind tunnel (VSW) is attached to the primary wind tunnel via a tower at the sand collector. A pair of shutters can open or close either of the tunnels permitting that the sand collector and the motor-fan units are utilized for both tunnels. The cross section of the VSW is smaller than that of the HW – only 0.35 m by 0.50 m. The length of the VSW is only 6 meters which for the ± 25° variation of slope (upslope and downslope) uses the full height of the laboratory. The front of the tower is covered with gates which, when moved one by one from below to above the tunnel (or vise versa), permits the slope of the tunnel to be varied in 5° bins. A small bell-mount is placed at the inlet as in the primary tunnel. The side panels of the tunnel is made of glass panes which cannot be opened. Access to the interior of the tunnel is limited to gates placed almost continuously in the tunnel ceiling between the entry and the tower. The working area is from 2 m to 5.5 m downstream of the entry. The VSW has a sand feed similar to that of the HW and sand is trapped in the common sand collector except during downslope experiments where most of the sand is trapped in a box at the bottom of the tower rather than in the sand collector.

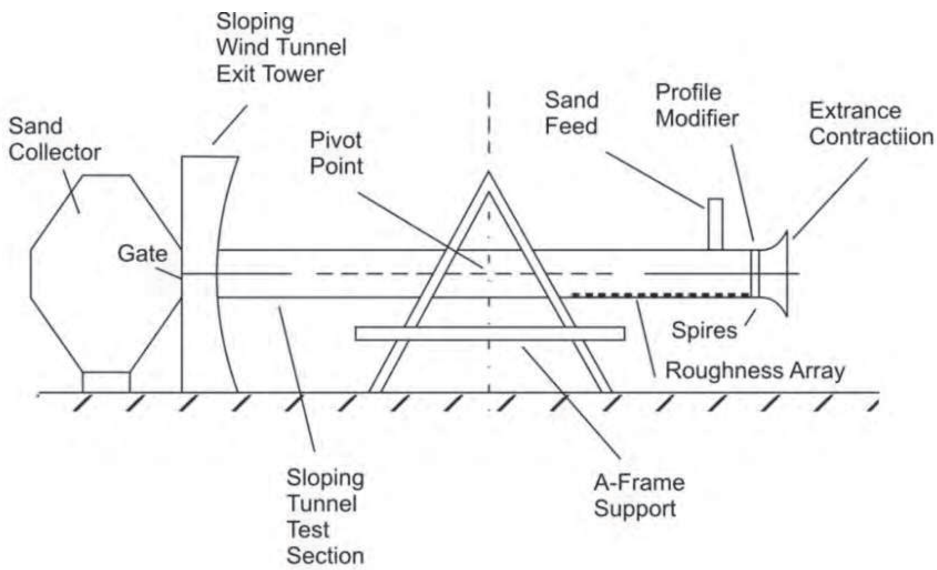

Fig. 7. Schematic diagram showing the sloping wind tunnel. The exit tower permits the slope of the tunnel to be varied in 5" increments from - 25" to +25". The tunnel is suspended in the A-frame with a pivot point at the center of symmetry. It is balanced by adjusting a counterweight with respect to its distance from the pivot point.

3.2 Boundary layer modification in the tunnels

When sand is introduced from the sand feed, it carries the momentum that is necessary for the chain reaction of saltating grains to create an equilibrium sand transport rate. However, both the horizontal and the sloping tunnel are too short and too shallow to allow the development of a natural boundary layer which is sufficiently deep and has turbulence characteristics equivalent to those above a sand surface in Nature. While the turbulent spectrum in a wind tunnel can never fully simulate that of the atmospheric boundary layer the average wind profile and the high frequency part of the spectrum can be artificially "designed" so that it makes a reasonable analogy to atmospheric surface layer flow. Therefore immediately downwind of the entry we aim to construct a wind flow which will be in fair equilibrium with the saltation boundary that develops downstream of the sand feed (figure 6 and 7).

Observations made in a previous, smaller wind tunnel indicated that for a high friction speed ($u^* \approx 1$ m/s) the aerodynamic roughness z_0 will increase by a factor of thousand as compared to the quiescent surface. For windblown quartz sand Rasmussen et al (1996) find that z_0 typically falls in the range 4×10^{-5} to 1.1×10^{-3} m when friction speed ranges between 0.2 m/s to 0.75 m/s. No single static roughness can therefore represent this enormous range in dynamic sand roughness. It has thus been considered necessary to create, with turbulence spires and roughness blocks, a boundary layer which for some selected friction speeds matches the dynamic saltation layer roughness and required boundary layer in the test sections of the two wind tunnels. We have selected nominal values of the friction speeds $u_* = 0.2, 0.3, 0.4, 0.6$ and 0.7 m/s u_* at which all experiments must be conducted, and in the next section we shall explain how spires and roughness blocks are used to control the state of the boundary layer.

Spires and roughness blocks

A thick boundary layer which assures dynamic similitude with natural surfaces of drifting sand and which permits measurements of the velocity profile is created with triangular turbulence spires which are inserted in the flow immediately after the bell-mouth. In our test section of height H_0, the shape of the log-linear wind profile is determined at the entry by the spire geometry i.e. spire height H, base width b and spacing L_s. We have aimed for a boundary layer thickness $\delta \approx 10$ cm at approximately 1 m downwind of the entry and the single steps in the design follows the procedure summarized by Irwin (1981). A spire design corresponding to $u_* = 0.40$ m/s is shown in fig. 8.

On the first 2.4 m of the test section between the spires and the fully developed saltation layer we control the boundary layer by an array of cubic roughness blocks, of block size h and spacing D. Somewhat subjectively we have preferred to base the roughness arrays on 3-dimensional roughness elements (Wooding, 1973) rather than 2-dimensional elements suggested by e.g. Gartshore, 1973).

Raupach et al. (1991) have proposed that for sparse roughness arrays

$$z_0/h = \lambda \tag{1}$$

where λ is aspect ratio (frontal area/areal block density). They find that $z_0/h|_{max} \approx 0.1$. Rather than using one block size for the entire set of nominal roughness values we use cubes with sizes of 10, 15, 20 and 25 mm placed in a cubic geometry and then control the particular roughness value by the λ-value. An array design corresponding to $u_* = 0.40$ m/s is shown in figure 8. One could point out, that Irwin's method gives higher values of the exponent n in the power law profile which is fitted to the boundary layer profile than suggested for example by Counihan (1975) but this is of minor importance because of the long working section.

Fig. 8. Turbulence spires and roughness array for a nominal friction speed of 0.4 m/s.

Fig. 9. The sand feed system.

3.3 Sand feed

In order to avoid depletion of sand from the upstream part of the bed sand must be supplied continuously during experiments. When the airflow is above the threshold of movement saltation is initiated through the collisional chain reaction governed by the splash function (Anderson and Haff, 1991). However, when the fetch is short, such as in a wind tunnel it is imperative that an external source initially supplies momentum to the saltation cloud in order to start the saltation process almost momentarily from nil to its fully saturated value. Although the range of particle size in wind-blown sands is usually narrow it also appears that the sand feed is necessary to stimulate transport until the friction velocity is above its threshold value for almost the entire grain population (Rasmussen and Mikkelsen, 1991). Otherwise the coarser grains in the sample will slowly armour the bed and reduce or even stop saltation transport.

The sand feed used for the VSW is only 350 mm wide while for the HW it is 600 mm (figure 9). However, the cross section of the two sand feeds is the same. Sand is stored in the upper funnel from where it drops into the grooves of a rotating drum which then carries the sand to the lower funnel. The lower funnel is divided into five chambers from where the sand slides into a 10 mm steel tube and then into the wind tunnel (visible above the roughness array on Fig. 8). Depending on the wind flow (friction speed) in the tunnel the tubes stop at 0.4 m above the wind tunnel floor ($u_* < 0.5$ m/s), at 0.2 m ($0.5 < u_* < 0.75$ m/s) or at 0.1 m above the wind tunnel floor (0.75 m/s $< u_*$). Thus for the higher friction speeds it is necessary to release the particles shortly above the bed in order to prevent them from being caught by the air flow and impacting with the bed at some distance within the working section where they will create a local scouring of the bed.

The speed of rotation of the drum is controlled with a potentiometer which allows the amount of sand being released from the sand feed to match fairly well the amount of sand leaving the tunnel in the downwind end. A calibration curve for the transport capacity as function of potentiometer setting is based on many experiments with quartz sand of different grain size distributions.

3.4 Sediment capture

The sand arriving to the sand collector at the downwind end of the tunnel is exposed to a sudden drop in wind speed because the cross sectional area expands by a factor of almost 10 when the wind flows from the tunnel into the centre part of the sand collector. One screen (S) halfway into the expansion (figure 6) results in some divergence of the flow from its jet-like behaviour when exiting the tunnel. The screen has a 50 % porosity and 100 micron holes so it catches most airborne grains. Because of the drop in speed between the exit and the screen grains then fall to the sloping part of the floor in the first part of the sand collector. Here a 5 mm gap between the screen and the wall allows the particles to slide down to bottom of the wall. Despite the overall drop in average speed in the collector, at high speed in the tunnel some of the finer grains in the collector are occasionally picked up from the floor by forceful eddies and swept around. Eventually they are caught by the screen with 50 micron openings which is placed halfway into the downwind exit of the sand collector. After an experiment both screens must be cleaned for particles which can then be brushed up from the floor.

3.5 Traps

Sediment transport rate in the tunnels is estimated in two different ways. The simple way to do it is to collect the total amount of sand arriving to the sand collector during an experiment and then estimate the average flux (ϕ_{SC}) of sand by normalizing it with the duration of the experiment and the width of the tunnel. A thin boundary layer of the order of 5 cm is present along each side of the tunnel. Here the transport rate is lower than that (ϕ_{IK}) measured along the centre line of the tunnel using an isokinetic trap (Rasmussen and Mikkelsen, 1991). However, a comparison of flux values measured in the two different ways show that independent of wind speed the ratio between the two quantities is fairly constant at $\phi_{IK} / \phi_{SC} = 1.16$.

An isokinetic trap, i.e. a trap through which air is flowing at the same speed as that of the surrounding air, is a more precise method for measuring the transport rate. The one that has been used for many years in the Aarhus wind tunnels has six 80 mm long compartments. Each compartment is made from brass tubes with a rectangular cross section. All compartments are 8 mm wide; the lower two are 4.5 mm high, while the other four are all 9.5 mm high (Fig. 10a). Each tube is sharpened at the leading edge so that the aperture facing the flow has a well-defined cross-section. Air is sucked through each tube at approximately the same speed as that of the undisturbed air flow upwind of the trap. The apertures are positioned at 60 mm upwind of the location where the tubes go through the bottom of the tunnel, thereby reducing the obstruction to the wind, even when the lowest tube is close to, or at, the sand surface. Because the lowest tube can be placed directly at bed level, particle creep is included in the transport rate measurements. The trap is adjusted carefully during experiments so that the bottom of the lowest compartment is always kept at the same elevation as the local sand surface. The vertical position of the sample tubes can be adjusted individually. Air drawn through the tubes goes through a container where the sand grains are trapped. The air exits by a nozzle valve with which we can adjust the flow rate through each tube to an accuracy of about 10% in the range 1.3-10 m s-1. The sample containers are weighed after each experiment (±10 mg), and then cleaned with compressed air.

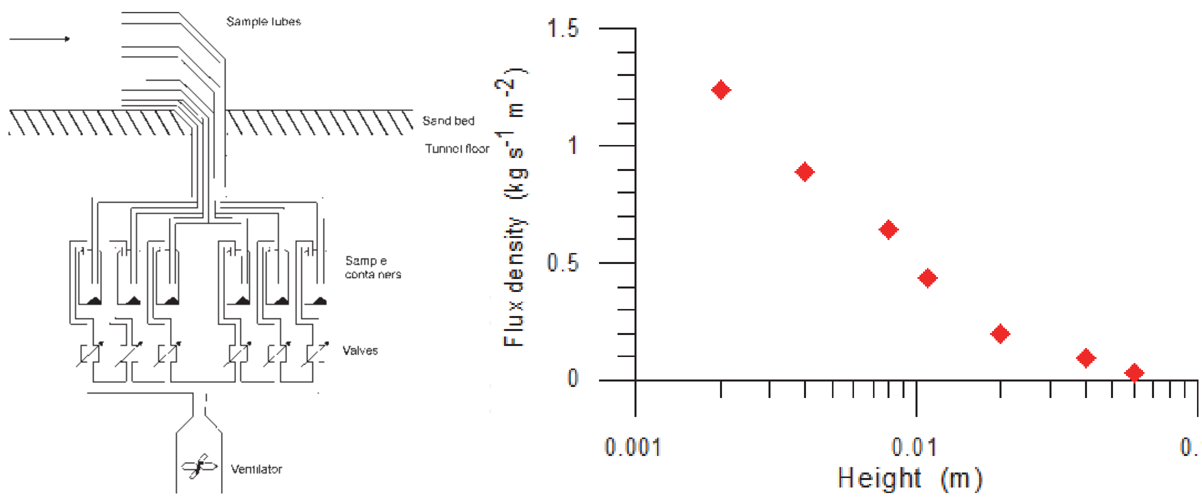

Fig. 10. **a)** Schematic view of the isokinetic trap with the suction flow control and six sample tubes; **b)** Flux-density profile measured with the isokinetic trap at a friction speed u_* = 0.49 m s^{-1}.

3.6 Air and grain velocity

In an aeolian wind tunnel the purpose of measuring speed is twofold requiring that the velocity of the air as well as the velocity of the particles is recorded. The bombardment of the sensor with saltating grains requires that only rather robust sensors can be used. Yet at the same time they must be small and very sensitive so that precise measurements at precise elevations can be made within the shallow wind tunnel boundary layer. A velocity sensor is usually fixed in space and therefore it will only record the instantaneous and local velocity of saltating grains. Information about the displacement of grains during the saltation process has also been attempted and will briefly be discussed, too.

For air speed we have mostly used a pitot static tube, but occasionally a robust hot wire has been used, too. A small diameter pitot-static tube (3/16" diameter) connected to a precision barometer is used to measure detailed wind profiles. The instrument measures the pressure difference between the dynamic and static pressures at a given location. Readings are typically taken at a frequency of 2-50 Hz depending on the duration and purpose of the experiment and then converted to instantaneous wind speed. The precise manometer readings combined with the high precision of the elevation at which the orifice of the pitot-static tube can be set, allows us to record quite detailed and precise wind speed profiles (figure 11). However, the pitot-static tube is sensitive to direction of the flow and it is mostly used in simple one- or two-dimensional flows which are parallel to the centerline of the wind tunnel.

A robust, omnidirectional steel clad hot wire (Dantec 55A76) connected to a constant temperature anemometer system (Dantec 55K01/) has occasionally been used to measure wind speed in the tunnel when flow conditions are complex so that the wind vector is not parallel to the axis of the wind tunnel. For any two-dimensional flow this sensor only needs to be placed with its support parallel to the invariant flow direction then it will always measure the local or instantaneous wind vector. Besides for wind tunnel studies with complex flows this also makes it a useful sensor for field studies.

Grain speed is measured using a one-dimensional laser-Doppler instrument with a flow velocity analyser (LDA, FVA, Dantec Floware). Mostly we use optics with a 400 mm focal length which allows measurements to be made from the outside with the beam pointing through the glass panes perpendicular to the direction of the flow. The beam height is 200 µm so it is possible to set precisely the height of the measurements. In the direction perpendicular to the flow the crossing between the two beams is just over 4 mm so the transverse position of the beam is much less well-defined. Irregularities of the bed and the increasing number of grains makes it difficult to come quite close to the bed and the movement of the ripples continuously changes the local elevation of the bed and therefore it is difficult in practise to acquire good quality data much closer to the bed than 2-4 mm (Rasmussen & Sørensen, 2008). Two examples of grain velocity profiles recorded with the LDA-equipment are shown in fig. 11.

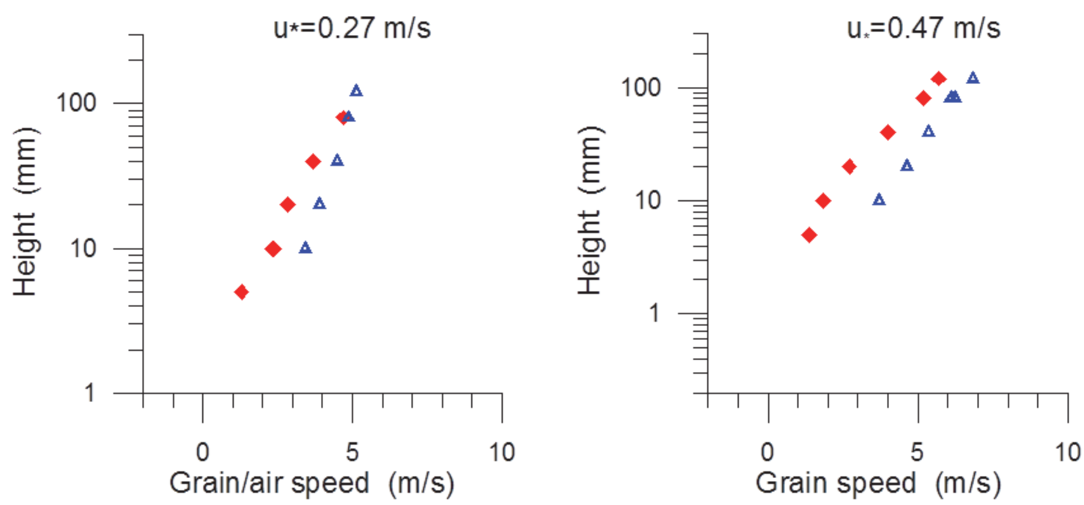

Fig. 11. Wind speed (blue triangles) measured in the horizontal wind tunnel above saltating 320 µm quartz sand (red diamonds) at two different friction speeds (u_*).

Finally we shall mention a few examples of techniques that have been applied to follow and measure the displacement of grains during active saltation. In the sand population approach one studies the transport characteristics of a whole population of sand grains. This may be done by dyeing samples (e.g. using Coomassie Brilliant Blue) of the grains and investigating how these are distributed by the wind along the wind-tunnel, the bottom of the wind-tunnel being covered in advance with a sand bed. The alternative individual approach to the question of the celerity of the grains consists in observation of the movement of single grains, which can be done, e.g. by labeling grains with radioactive gold. The element gold is an obvious choice for the following reasons: it has a very high neutron activation cross section and the radioactive product, ^{198}Au, has a suitable half-life (2.7 days) and emits gamma-rays of a convenient energy (412 keV). However, the adhesion of gold to quartz is poor, but this problem can be solved by covering the quartz with a thin chromium layer first. Then the gold will stick so well that it is almost impossible to rub it off. So first we have coated sand grains with a layer of chromium metal, 10nm thick, by evaporation in high vacuum. Then a layer of gold metal, 250 nm thick, is evaporated onto the grains. These layers are so thin that the coating will result in an insignificant change of mass, typically 1-2% of the total mass of the grain. The position of two radioactive grain marked as described above was determined by means of a portable scintillation detector (for more information see Barndorff-Nielsen et al, 1985). During both wind tunnel experiments the bed of the tunnel was covered with a 1.5 cm thick layer of sand. The wind speed was between 7.0 and 7.5 ms^{-1} in the center of the tunnel. In each run a single radioactive grain was placed 8.0-8.5 m from the intake of the tunnel and followed during its movement. The recorded movements of two of the marked grains from the pilot experiment are shown in figure 12. Time in minutes is indicated on the abscissa, while the ordinate gives the distance travelled, in m. The experiment clearly shows that a sand grain is buried rather often while a ripple passes over it. However, the grain is not in constant motion while it is not buried. It is at rest on the surface for a period; then it is launched – either directly by the wind or by another grain that hits it – and makes a jump or a number of jumps in immediate succession. The duration of a period of motion is negligible compared to the waiting times, except for a few of the smallest grains. Grain No. 6 was, apparently, never or only a few times buried under a passing ripple for some rather long periods.

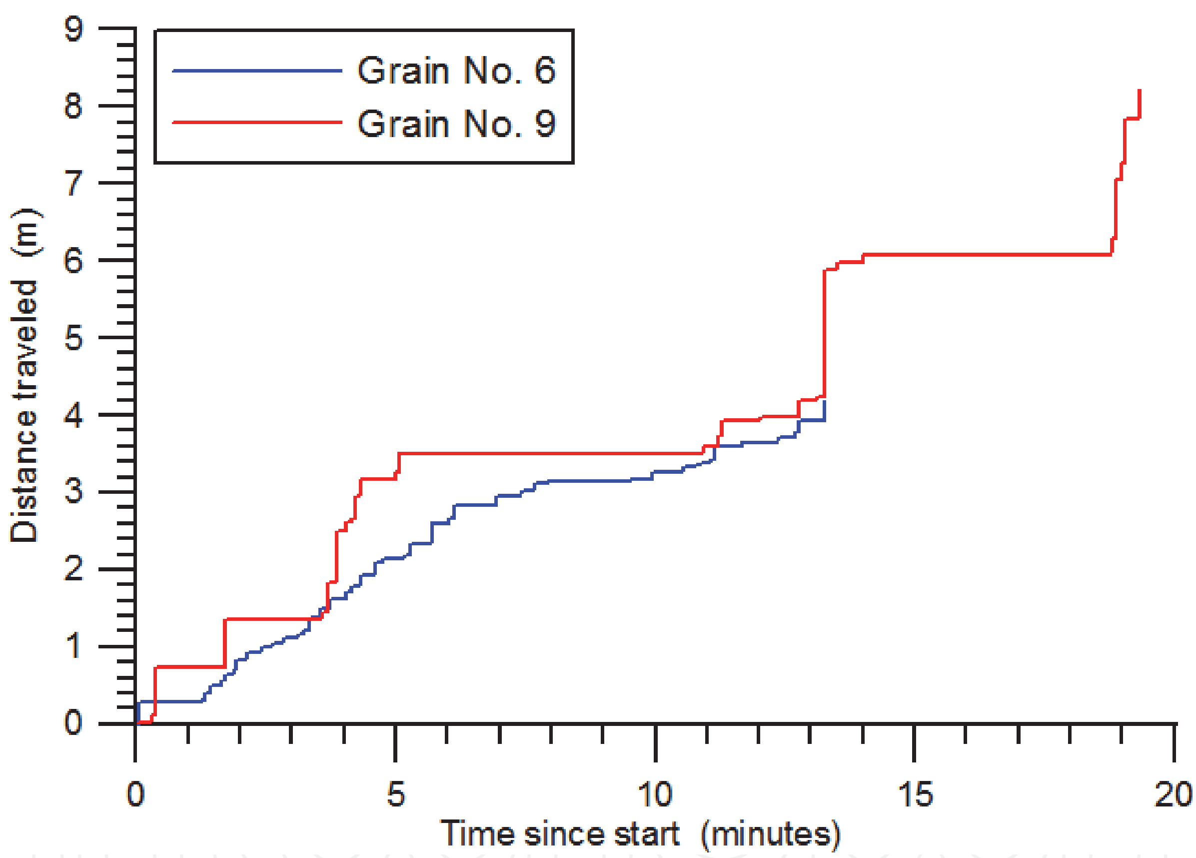

Fig. 12. Movement of two radioactively marked grains during saltation.

3.7 Electric field

A uniform electrical field can be created in the entire working section of the horizontal wind tunnel by suspending all the way down the working section a set of 10 parallel steel wires. The wires are made of 0.3 mm piano string and suspended at 80 mm height above the bed thereby creating one electrode with a constant distance to the bed. The inside of the (wooden) wind-tunnel bed has been painted using a conductive paint in this way forming another electrode just below the sand bed. The two electrodes can then be connected to the positive and negative terminals of a high voltage supply unit enabling us to study saltation under the influence of an electric field (Rasmussen et al. 2009).

4. Low pressure wind tunnels for aerosol studies

4.1 Planetary environmental wind tunnels

The wind tunnel laboratory at Aarhus University has developed two wind tunnels for planetary surface experiments. The smaller one has a test section 40 cm in diameter and about 50cm in length (Merrison et al. 2002, Merrison et al. 2008). The larger wind tunnel has a test section of around 2 x 2 x 1 m. In these environmental wind tunnel facilities dust suspension and aerosol studies can be performed. They are both re-circulating wind tunnels housed within low pressure (vacuum) vessels such that they can be evacuated and specific gas mixtures re-pressurized. Pressures in the range 0.01mbar and 1000mbar can be maintained. In addition a thermal control system has been constructed which consists of an insulated double walled chamber design. The cooling and fan systems are different in the two wind tunnels and we will here focus on the bigger wind tunnel (AWTSII). An exploded view of this is seen in figure 13a.

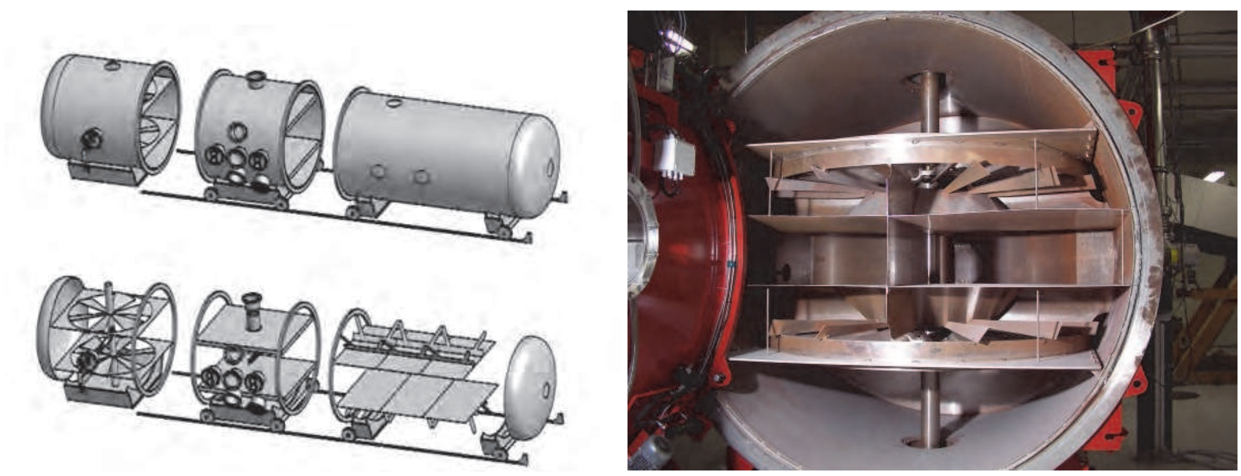

Fig. 13. a) Exploded view of the AWTSII planetary environmental wind tunnel, and b) photograph into the fan section.

The wind tunnel has large liquid nitrogen cooled sample mounting platforms. The wind circulation is achieved with the use of two 1.8m diameter fans and intricate flow steering plates (figure 13b). The wind flow is designed such that an almost rectangular test section is provided, though at the cost of a relatively complex two part flow return system. Turbulence levels, however, are maintained at around 5-15% (typical of Martian surface conditions). The wind tunnel test section has a cross section of around 1 m height and 2 m width and with a length of around 7 m. Wind speeds of around 0.5 – 20 m/s have been demonstrated at low pressure (<100mbar). The wind tunnel simulator has been designed with the goal of maintaining dust suspension (or other aerosol types), such that low turbulence and flow uniformity have been prioritized lower than allowing as little obstruction of the flow as possible to avoid deposition losses. The design therefore differs from boundary layer wind tunnels or those aimed at low turbulence (laminar flow).

4.2 Dust aerosol generation

A necessary process for the study of aerosols in the laboratory is the generation of suspended particulates within a simulator. In the case of solid particulates (dust) this will involve the dispersion of the fine material which will typically be in the form of aggregates.

The most effective and reliable method for aerosol generation consists of the injection of over-pressurized gas together with the required granular material such that a rapid expansion of the gas-particulate mixture causes dispersion of individual dust grains (Merrison et al. 2008). In the case of wind tunnels the high instantaneous wind speed at the injection nozzle also helps to distribute the aerosol into the wind flow. Essentially the same technique is used to generate aerosols consisting of liquids, for example water. In this case fine streams of liquid are mixed with gas (air) flow at an expansion nozzle such that the high velocity and turbulent gas flow disrupts the liquid and disperses it into individual particulates. In this way liquid particulates as small as a micrometer can be generated. With the use of controlled overpressure and quantified volumes/mass of injected gas and dust material it is possible to achieve reproducible dust aerosols i.e. controlled concentration of suspended dust within the wind tunnel simulator.

In nature the wind induced entrainment of dust occurs as a result of surface shear stress which above a certain threshold value is capable of overcoming adhesion and gravitation and lifting particulates. The low mass density of (sand sized) dust aggregates allows them to be entrained at wind speeds lower than other granular materials (shear stress). Subsequent breakup of the dust aggregates may liberate dust grains into suspension (Merrison et al. 2007). At higher wind shear solid sand grains may be entrained and perform saltation. Sand saltation is also an effective process capable of entraining dust due to collisional recoil i.e. during sand grain splash (Greeley and Iversen 1985).

A drawback with the gas-expansion technique for dust injection is that it is unlike the dust entrainment mechanism found in nature and therefore may not be directly comparable. It has been shown experimentally that wind induced dust entrainment can be used as a dust injection method within a re-circulating wind tunnel. This technique relies on accumulating a thick deposited dust layer within the wind tunnel, possibly localised to a particular section. Entrainment can then be performed by raising the wind speed temporarily above the threshold entrainment value. After achieving dust suspension the wind speed can then be reduced to the required value. This technique is effective, though it is difficult to perform in a reproducible manner i.e. to achieve a specific entrained dust concentration. For the quantitative study of aerosols, reproducibility is of primary importance making this technique unsuitable as a routine dust injection method.

The threshold wind speed at which dust becomes entrained is dependent upon several factors. Dust particulates of the order of a micrometer in size require extremely large surface wind shear to be entrained as individual grains. Dust however tends to aggregate into structures of the same scale as sand grains i.e. several hundred micrometers. Such aggregated dust structures have a low mass density (typically $<1 g/cm^3$) and can be removed by surface shear stress as low as 0.01 N/m^2 corresponding to friction velocities as low as 0.1 m/s at ambient terrestrial pressure (Merrison et al. 2007). This is significantly lower than that required for sand transport.

Other methods of dust injection have been studied, for example techniques which rely on mechanical (e.g. vibrational) dispersal of dust. Unfortunately a fundamental problem with this type of dust dispersal system, also seen generally in dust feeding systems, is the tendency of dust to become compacted, adhered and cause blockage. To avoid such blockages it may be possible to keep the dust fluidized by maintaining a high gas content i.e. mixing or flowing gas through the dust, however this tends again to return to an injection system utilising pressurized gas-flow.

A physical phenomenon which has great importance to the behaviour of aerosols is the electrification of particulates as a result of contact. Contact electrification is seen widely both in nature and anthropological activities where granular materials interact, for example Aeolian transport (Stow 1969, Gilbert et al. 1991, Schmidt et al. 1999). Extensive experimental studies have revealed that the injection of dust induces a high level of particulate electrification, typically resulting in the suspension of equal amounts of positive and negative electrified dust grains (Merrison et al. 2004a). This electrification leads to the electrostatic enhancement in dust aggregate formation and may be an important factor in the transport of dust, specifically in dispersal/detachment and suspension/deposition. Following injection aggregation of dust leads to reduction of the electrification of the suspended dust. The degree of electrification of the suspended dust decreases with time and is therefore dependent upon the concentration of dust. Since the suspension time of the dust is dependent upon the wind speed, the measured electrification of dust also varies with wind speed.

4.3 Dust suspension

Aerosols, for example suspended dust particulates, are not stable within a re-circulating wind tunnel. Processes such as gravitational deposition (settling), adhesion and aggregation lead to loss of suspended dust and reduction of the suspended number density. Typically the suspended dust concentration falls exponentially with time after injection. The time constant for this process is dependent upon the wind speed. At high wind speeds (>1m/s) dust deposition appears to be dominated by collision of dust particles with surfaces within the wind tunnel, leading typically to the accumulation of dust on wind facing surfaces. This gives a reduction in the suspension time with increasing wind speed. At wind speeds of around 10m/s the dust suspension time within the AWTSII facility has fallen to around 30seconds.

As mentioned earlier at wind speeds above around 7m/s, depending on the pressure, thick depositions of dust (dust aggregates >50μm) can lead to the wind shear induced re-suspension of deposited dust. At these high wind speeds and given large amounts of dust within the wind tunnel both dust suspension and deposition can occur at the same time making dust concentration a complex function. At the lowest wind speeds (around 1m/s) gravitational settling appears to dominate the deposition rate and the dust suspension time becomes independent of wind speed. In the case of AWTSII this suspension time is around 300 seconds at around 15 mbar (i.e. Mars simulation conditions) in agreement with estimated gravitational settling time. Dust suspension as described above is relevant for dust grains of the order of a few micrometers in size and bulk mass density of up to a few thousand kg/m^3. Larger or denser dust grains will typically lead to decreased suspension times due to enhanced gravitational deposition. This will naturally lead to a mineral (compositional) dependence of dust suspension time as a result of variation in grain size, morphology, mass density and possibly cohesiveness (difficulty in dispersion). Higher gas mass density within the wind tunnel will also allow increased aerodynamic drag and therefore increased dust suspension times. However wind tunnel pressure may also affect the dust injection system, specifically the gas-expansion system will become inefficient at reduced pressure differential.

It is useful here to present a basic fluid dynamic relation relevant to the suspension of dust particulates within a (low pressure) wind tunnel. For dust particulates of the order of a few

microns Stokes relations will be valid as indicated by the low Reynolds number (<0.1). Dust grains can typically be assumed to follow the fluid flow well (the same wind speed and turbulence). Under the action of external forces (F) such as gravitation, electrostatic or magnetic affects, the particulates can be assumed to accelerate within a short period of time (<<1s) and therefore given a uniform field achieve terminal velocity, that is to say reach a drift velocity at which the external force is balanced by the drift induced drag (U_T) (Hall 1988, Fay & Sonwalker 1991). Values of the electric field induced drift velocity U_T have typically been calculated to be around 1cm/s for fields of order 10KV/m.
The value of this terminal velocity is given in equation 1;
Equation 1 (field induced drift velocity); $\boldsymbol{U_T} = \boldsymbol{F} \times \frac{S}{6\pi\mu r}$
Here μ is the molecular viscosity (for air $\mu = 1.8\times10^{-5}$ kg/ms) and r is the dust grain radius.
At the low pressures used in most Mars simulation studies the suspended particulate size is smaller than the collision distance between gas molecules (the scattering length, λ). Here an empirical relation can be used to correct for the non uniform nature of the gas, called the slip factor; $S = 1 + \frac{\lambda}{r}\left(1.257 + 0.4 \cdot \exp(-1.1\frac{r}{\lambda})\right)$. This factor is of the order of 10 in most Mars simulation studies, though is typically negligible at ambient pressure.
The simplicity of this relation allows the accumulation of dust within a wind tunnel environment to be used to quantify (estimate) the force(s) applied to the dust particulates. This simplicity however relies on the assumption of average particulate properties such as size, mass, morphology as well as the external forces applied. It also neglects effects of the flow such as turbulence.

4.4 Dust deposition

At low turbulent flows dust deposition is dominated by gravitational settlement as turbulent wind speed is small compared to the gravitational terminal velocity. In this case dust deposition within a wind tunnel will be dominated by settlement onto upward facing surfaces. At higher wind turbulence it becomes more likely that suspended grains can impact surfaces and deposition on wind facing surfaces begins to occur. This process of dust deposition is dependent upon details of the boundary layer flow around surfaces within the wind tunnel. This near surface boundary layer is conventionally divided into two regions. A region close to the surface within which the flow velocity increases linearly from zero (at the surface) and shear stress is transferred by viscous interaction. Outside this region turbulence becomes dominant as the mechanism for transferring shear stress and the flow velocity increases logarithmically. The transfer of stress through turbulence occurs through variations in the properties of macroscopically sized volumes of the fluid. Turbulence is a fundamental property of fluids and related to variations in velocity, pressure, temperature, etc. Turbulence occurs on all spatial and temporal scales above the molecular level (Monin & Yaglom 1973.) The concept of an ideal viscous region (of molecular flow) at the surface is likely to be a simplification and at odds with the inherently statistical nature of turbulence such that in reality suspended particulates can still be transported to a surface though with low probability.
At higher wind shear the boundary layer is expected to shrink (spatially) and the turbulence is expected to increase in agreement with the observed increase in surface impacts by suspended grains. It is interesting here to note that increased dust deposition (due to high turbulence) and increased dust removal (due to high surface shear stress) can occur, and in fact is expected, at the same regions within the wind tunnel.

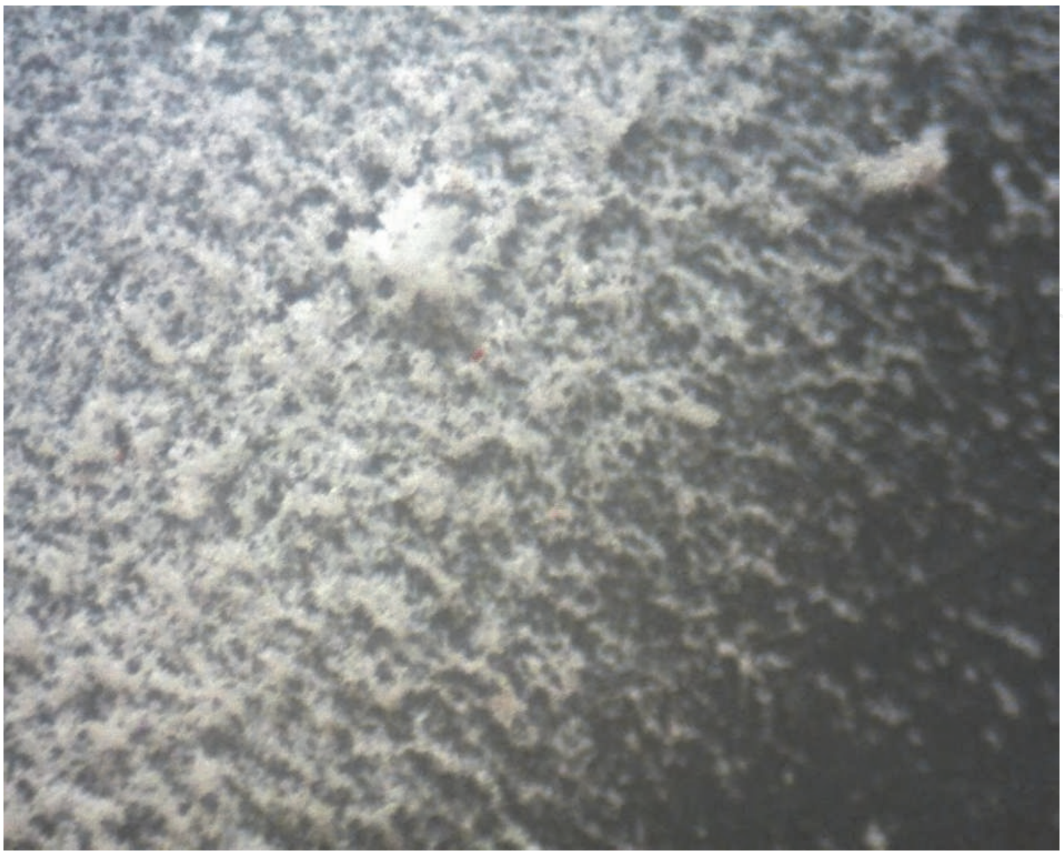

Fig. 14. Aggregated quartz grains (<2μm) deposited on an upward facing surface after wind tunnel aerosol exposure.

4.5 Dust capture and sensing

Experimentally it is useful to collect suspended dust onto a surface. This could be for use in compositional or structural analysis or for the determination of concentration. It is not always sufficient to rely on gravitational or turbulent deposition of dust either because of the amount of material required or the flow conditions. Methods of enhancing dust accumulation include applying (attractive) force to the particulates. This could involve the use of electrical or magnetic fields in the case of electrified or magnetic particulates. This technique has been used to great effect to study the electrical/magnetic properties of suspended dust on Mars and in wind tunnel simulators. An alternative technique which is used industrially and in environmental sciences is the use of a pump system to extract specific volumes of gas. Suspended particulates can then be accumulated within filters or onto surfaces. Such systems have not as yet been used in wind tunnel studies, however an important application of wind tunnels is in the testing and calibration of environmental sensors and it seems likely therefore that wind tunnels will be used for this purpose in the future.

Different techniques can be used to quantify the amount of dust captured onto a surface. Microbalances can be used to determine the accumulated mass (and therefore mass density) of the suspended dust, this however requires a high degree of detector sensitivity. Alternatively optical systems could be used to quantify dust deposition. This could involve the use of imaging or the reflection/transmission of light using optoelectronic systems. Optical (also laser based) systems have been used successfully here (Merrison et al. 2006).

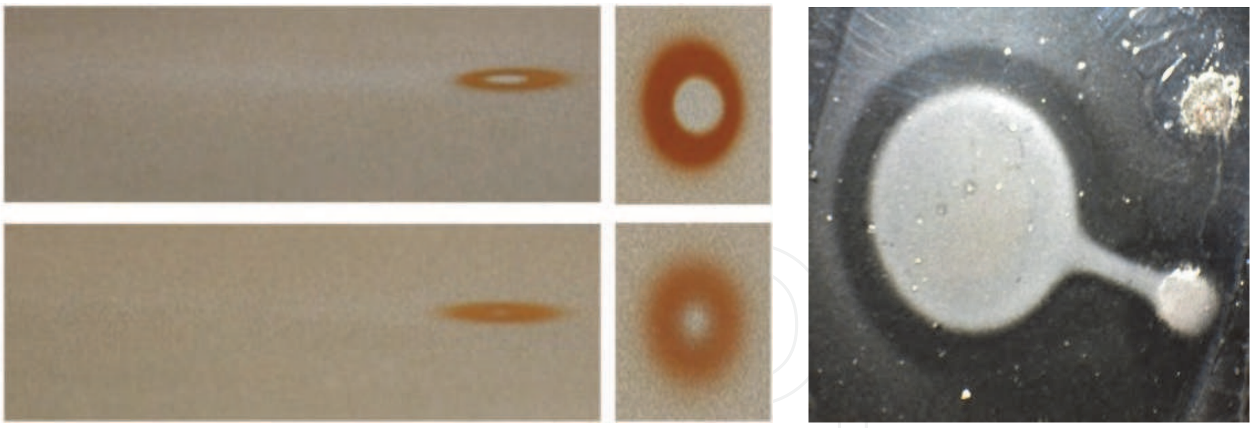

Fig. 15. Left dust capture on a NASA Phoenix camera calibra-tion-target magnets and a model of the MSL calibration-target magnets for uni-directional wind. Right quartz dust capture on an electrostatic electrode (voltage 300V).

4.6 Suspended dust sensing

The scattering of light by suspended particulates is the obvious and by far the most widespread technique for studying suspended dust aerosols. Modern techniques which are applied in meteorology include determination of the optical opacity (scattering of sun light). Such measurements tend to be simple to carry out, however detailed modelling of angular scattering intensities are required to determine suspended grain size, morphology and concentration. More advanced and direct systems for determining the spatial distribution of dust aerosols include the laser based technique LIDAR which is successful both commercially and in research for example in the study of clouds. This technique is, however, not well suited for wind tunnel operation.

Within wind tunnels other laser based techniques are used to study dust aerosols. Laser Doppler Anemometers (LDA) are primarily used for wind velocity sensing. They function by scattering light from suspended particulates and hence have the added benefit of being able to quantify the aerosol concentration (number density) typically for particulates of above around one micron. Further modifications of LDA systems enable the spatial distribution (multiple dimensions) and grain size to be quantified. In addition to such commercial sensor systems prototype (miniaturized) instruments are being developed in order to detect suspended dust and measure flow rates (Figure 16) (Merrison et al. 2004b, Merrison et al. 2006).

5. Modelling

Computational Fluid Dynamic modelling is in principle a useful technique for identifying and solving problems with the design of a wind tunnel by detailing the wind flow. It is however extremely time consuming (compared to typical measurement and even construction time scales) especially if three dimensional modelling is employed (Peric and Ferziger 1999). CFD models are also prone to inaccuracies resulting from insufficiently high time/space resolution (pixelisation). A combination of measurement and modelling is however a powerful combination to achieve a full understanding of the flow dynamics within a system (Kinch et al 2005).

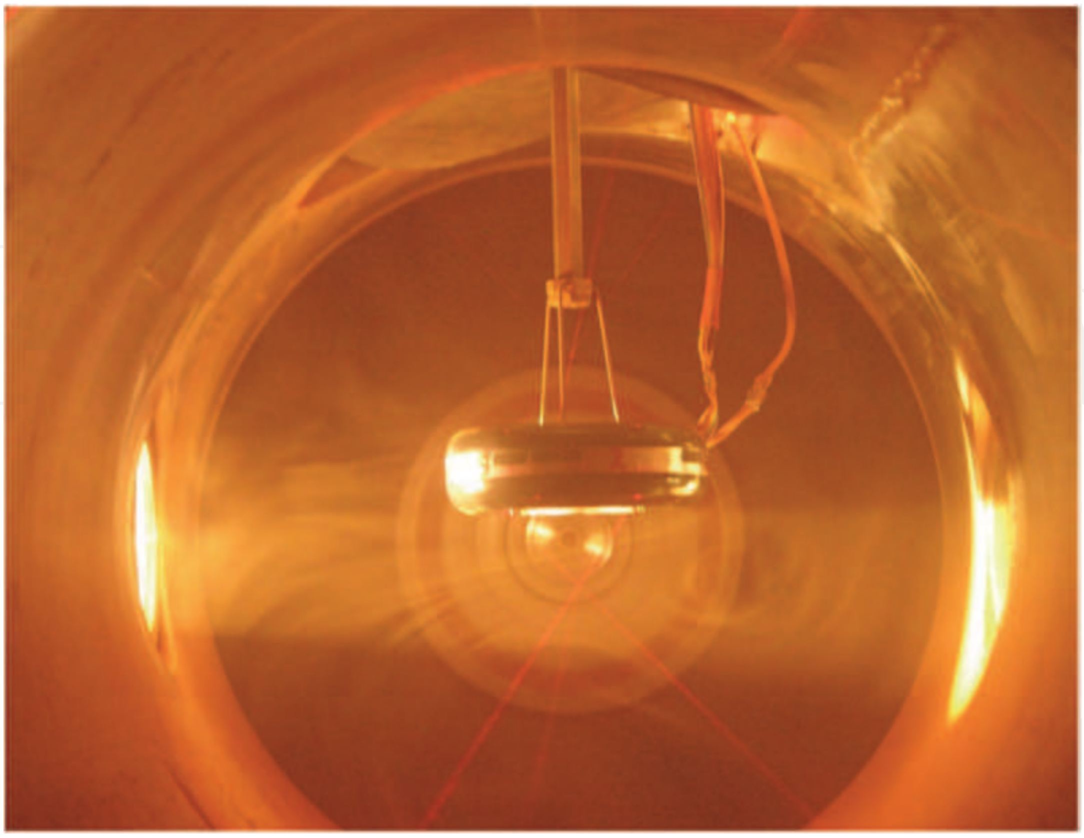

Fig. 16. Prototype laser based sensor system operating in a dust aerosol within the 40 cm Ø diameter environmental wind tunnel.

As explained in the preceding sections there are fundamental differences in the physics that control the movement of sand and dust. Therefore the approach to model (analytically or numerically) the transport of dust and sand follows different principles. In aeolian transport, saltation is an important link by which momentum is transmitted from the air to the bed through grain impact, but momentum transfer, impact and subsequent entrainment take place in a very shallow layer at the air-bed interface with large velocity gradients. Consequently, in addition to experimental evidence obtained from few and simplified studies of the splash (e.g. Willetts & Rice 1986, 1989, Mitha et al. 1986) theoretical reasoning and numerical modelling has played an important role (e.g. Owen 1964, Sørensen 1985, Anderson & Haff 1988, 1991, McEwan & Willetts 1991, 1993, Shao & Li 1999, Spies & McEwan 2000). After the sand grains have left the surface they are accelerated by the wind with trajectories influenced by fluid drag, gravity, particle spin and fluid shear, and electric forces. This process has been modeled by several authors (e.g. Anderson & Haff 1991, McEwan & Willetts 1991, Sørensen, 1991, Sørensen 1995, Sørensen 2005 and Kok and Renno 2009). The physics governing the splash, the grain trajectories and the momentum exchange between the fluid flow and saltating particles has been specifically formulated in the models mentioned above and is not traditionally dealt with in a CFD-context.

For aerosols where with CFD modelling it is possible to inject virtual particulates within the flow and trace their transport. It may then be possible to apply external force fields (gravitational, electrostatic or magnetic) and thereby perform a faithful reconstruction of the physical conditions within the wind tunnel. In this case an extremely detailed physical description of an observed phenomenon can be obtained and therefore the dependency upon for example grain size, mass, electric charge, magnetisation, etc. Also physical parameters not easily varied in laboratory experiments may be modelled such as varying gravity (Kinch et al. 2005).

6. Acknowledgements

The authors would like to thank the Villum Kann Rasmussen Foundation, the Villum Foundation, the Danish Science Research Council and the European Space Agency (ESA) (Contract No. 21285/08/NL/GLC) for finansial support to building of wind tunnels and instruments.

7. References

Anderson, R.S. & Haff, P.K. (1991) Wind modification and bed response during saltation of sand in air. In O.E.Barndorff-Nielsen & B.B.Willetts(Eds) *Acta Mechanica Suppl*. 1, 21-51.

Bagnold, R.A. (1941) The physics of blown sand and desert dunes. Methuen, London.

Beuselinck, L.; Govers, G.; Poesen, J.; Degraer, G.; Froyen, L. (1998) Grain-size analysis by laser diffractometry: comparison with the sieve-pipette method. *Catena*, 32, 193-208.

Chepil, W.S. (1959) Equilibrium of soil grains at the threshold of movement by wind, *Soil Science Society of America Proceedings*, 422-428.

Counihan, J. (1975) Adiabatic atmospheric boundary layers: A review and analysis of the data from the period 1880-1972. *Atmospheric environment*, Vol.9, 871-905.

Esthel, G.; Levy, G.J.; Mingelgrin,U.; Singer, M.J. (2004) Critical Evaluation of the Use of Laser Diffraktion for Particle-Size Distribution Analysis. *Soil Science Society America Journal*, 68, 736-743.

Fay, J.A. & Sonwalkar, N., (1991) "Fluid Mechanics", MIT, Boston.

Gartshore, I.S. (1973) A relationship between roughness geometry and velocity profile for turbulent boundary layers. National Establishment of Canada, Report LTR-LA-140.

Gilbert, J.S., Lane, S.J., Sparks, R.S.J., Koyaguchi, T. (1991) *Nature* 349, 598.

Greeley, R. & Iversen, J.D. (1985) Wind as a Geological Process on Earth, Mars and Venus. Cambridge Planetary Science Series. Cambridge University Press, Cambridge.

Greeley, R.; White, B.R.; Pollack, J.B.; Iversen, J.D.; Leach, R.N. (1981) Dust storms on Mars: Considerstions and simulations. In Péwé, T., editor, Desert Dust: Origin, Characteristics, and Effect on Man, *Geological Society of America Special Paper*, 186, pp.101-21.

Hall, D. J. (1988) Fluid Mechanics. 187, 451-466.

Irwin, H.P.A.H. (1981) The design of spires for wind simulation. *J. Wind Eng. Industrial Aerodynamic*, 7, 361-366.

Iversen, J.D. & Rasmussen, K.R. (1999) The effect of wind speed and bed slope on sand transport. *Sedimentology* 46, 723 -731.

Iversen, J.D. and Rasmussen, K.R. (1994) The effect of surface slope on saltation threshold. *Sedimentology*, 41, 721-728.

Iversen, J.D., Greeley, R., Marshall, J.R. and Pollack, J. (1987) Aeolian saltation threshold: effect of density ratio. *Sedimentology* 34, 699-706.

Iversen, J.D., Greeley, R. and Pollack, J.B. (1976) Windblown dust on Earth, Mars and Venus. *The Journal of the Atmospheric Sciences* 33, 2425-2429.

Iversen, J.D. and White, B.R. (1982) Saltation threshold on Earth, Mars, and Venus. *Sedimentology* 29, 111-119.

Kinch, K. M. Merrison, J.P., Gunnlaugsson, H. P., Bertelsen, P. Madsen, M. B., Nørnberg, P. (2005) Preliminary analysis of the MER magnetic properties experiment using a CFD model. *Planetary and Space Science.* 54, 28-44.

Klute A. (1986) Methods of Soil Analysis, Part 1, Physical and Mineralogical Methods, *SSSA Book Series*,

Madison, Wisc. USA.

Krumbein, W.C. ; Pettijohn, F.J. (1938) Manual of sedimentary petrography. Appelton-Century-Crofts, N.Y.

Marlow, J.J.; Martins, Z.; Sephton, M.A. (2008) Mars soil analogues. *Astronomy and Geophysics*, 49, 2, 2.20-2.23.

Merrison, J.P., Bechtold, H., Gunnlaugsson, H., Jensen, A., Kinch, K., Nornberg, P. and Rasmussen, K. (2008) An Environmental Simulation Wind Tunnel for Studying Aeolian Transport on Mars, *Planetary and Space Science,* 56, 426-437.

Merrison, J.P., Gunnlaugsson, H.P., Nørnberg, P., Jensen, A.E., Rasmussen, K.R. (2007) Determination of the Wind Induced Detachment Threshold for Granular Material on Mars using Wind Tunnel Simulations, *Icarus*, 191, 568-580.

Merrison, J.P., Gunnlaugsson, H.P., Kinch, K., Jacobsen, T.L., Jensen, A.E., Nørnberg, P., Wahlgreen, H. (2006) An integrated laser anemometer and dust accumulator for studying wind induced transport on Mars, *Planetary and Space Science,* 54, 1065-1072.

Merrison, J.; Jensen, J.; Kinch, K.; Mugford, R.; Nørnberg, P., (2004a) The electrical properties of Mars analogue dust, *Planetary and Space Science*; 52: 279-290

Merrison, J.P.; Gunnlaugsson, H.P.; Jensen, J.; Kinch, K.; Nørnberg, P.; Rasmussen, K.R. (2004b) A Miniature Laser Anemometer for Measurement of wind speed and dust suspension on Mars, *Planetary and Space Science*; 52(13): 1177-1186.

Merrison, J.P.; Bertelsen, P.; Frandsen, C.; Gunnlaugsson, H.P.; Knudsen, J.M.; Lunt, S.; Madsen, M.B., Mossin, L.A.; Nielsen, J.; Nørnberg, P.; Rasmussen, K.R. ; Uggerhøj, E. J. (2002) Simulation of the Martian Aerosol at Low Wind Speed. *J. Geophysical Research-Planets*, 107, 5133-5141.

Monin, A.S. & Yaglom, A.M. (1973) Statistical Fluid Mechanics: Mechanics of Turbulence Volume 1, MIT Press.

Morris, R.V.; Golden, D.C. Ming, D.W.; Shelfer, T.D.; Jørgensen, L.C.; Bell III, J.F.; Graff, T.G.; Mertzman, S.A. (2001) Phyllosilicate-poor palagoniteic dust from Mauna Kea Volcano (Hawaii): A mineralogical analogue for magnetic Martian dust? *Journal of Geophysical Research-Planets*, 106, E3, 5057-5083.

Moroz, L.V.; Basilevsky, A.T.; Hiroi, T.; Rout, S.S.; Baither, D.; van der Bogert, C.H.; Yokovlev, O.I.; Fisenko, A.V.; Semjonova, L.F.; Rusakov, V.S.; Khramov, D.A.; Zinovieva, N.G.; Arnold, G.; Pieters, C.M. (2009) Spectral properties of simulated impact glasses produced from martian soil analogue JSC Mars-1. *Icarus*, 202, 336-353.

Nørnberg, P.; Gunnlaugsson, H.P.; Merrison, J.P.; Vendelboe, A.L. (2009) Salten Skov I: A Martian magnetic dust analogue. *Planetary and Space Science*, 57, 628-631.

Nørnberg, P.; Schwertnamm, U.; Stanjek, H.; Andersen, T.; Gunnlaugsson, H.P. (2004) Mineralogy of a burned soil compared with four anomalously red Quaternary deposits in Denmark. *Clay Minerals*, 39, 85-98.

Nørnberg, P. (2002) Particle comminution and aeolian addition in young dune sand soils. *Transactions, 17th. World Congress of Soil Science*, Bankok, Thailand, Symp. No 25,Paper no 1124.

Owen, P.R., 1964. Saltation of uniform grains in air. Journal of Fluid Mechanics 20, 225-242.

Peric, M. & Ferziger, J.H. (1999) Computational Methods for Fluid Dynamics, Springer, 2 Ed.

Pettijohn F.J. (1957) *Sedimentary Rocks*, Harper and Row, N.Y

Rasmussen, K.R., Kok, J.F., Merrison, J.P. (2009) Enhancement in wind driven sand transport by electric fields, *Planetary and Space Science*, 57, 804-808.

Rasmussen, K.R. & Sorensen, M. (2008) Vertical variation of particle speed and flux density in Aeolian saltation measurement and modeling, *J. Geophysical Research- Earth Surface* 113(F2), F02S12.

Rasmussen, K.R., Iversen, J.D. and Rautaheimo, P. (1996) Saltation and wind flow interaction in a variable slope wind tunnel. *Geomorphology*, 17, 19-28.

Rasmussen, K.R. & Iversen, J.D. (1993) A variable slope wind tunnel for testing wind-blown sand. Proc. 7th U.S. National Conference on Wind Engineering. Vol. 2, pp. 643-552. University of California at Los Angeles.

Rasmussen, K.R. and Mikkelsen, H.E. (1991) Wind tunnel observations of aeolian transport rates. In: O.E. Barndorff-Nielsen and B.B. Willetts (eds) *Acta Mechanica, Suppl*. 1, 135-144.

Raupach, M.R. (1991) Saltation Layers, Vegetation Canopies and Roughness Lengths. In O.E.Barndorff-Nielsen & B.B.Willetts(Eds) *Acta Mechanica Suppl*. 1, 135-144.

Scheffer & Schachtschabel (1998) Lehrbuck der Bodenkunde, Ferd. Enke Verlag, Stuttgart.

Stow, C.D. (1969) *Weather* 24, 134.

Schmidt, D.S., Schmidt, R.A., Dent, J.D. (1999) Electrostatic force in blowing snow. *Boundary-Layer Meteorology*, 93 (1), 29–45.

Tanner, W.F. (1969). The particle size scale. *Journal of Sedimentary Petrology*, 39,2, 809-812.

Ulery, A.L. & Drees R. (2008) Methods of Soil Analysis, Part 5 – Mineralogical Methods, *SSSA Book Series*, Madison Wisc. USA.

Williams, G., (1964) Some aspects of the eolian saltation load. *Sedimentology* 3, 257-287.

Wooding, R.A., Bradley, E.F. and Marshall, J.K. (1973) Drag due to regular arrays of roughness elements of varying geometry. *Boundary-Layer Meteorology* 5, 285-308.

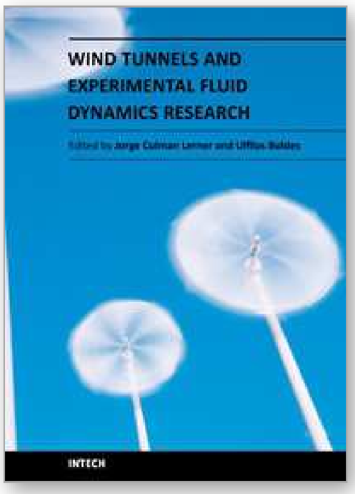

Wind Tunnels and Experimental Fluid Dynamics Research
Edited by Prof. Jorge Colman Lerner

ISBN 978-953-307-623-2
Hard cover, 709 pages
Publisher InTech
Published online 27, July, 2011
Published in print edition July, 2011

The book â€œWind Tunnels and Experimental Fluid Dynamics Researchâ€ is comprised of 33 chapters divided in five sections. The first 12 chapters discuss wind tunnel facilities and experiments in incompressible flow, while the next seven chapters deal with building dynamics, flow control and fluid mechanics. Third section of the book is dedicated to chapters discussing aerodynamic field measurements and real full scale analysis (chapters 20-22). Chapters in the last two sections deal with turbulent structure analysis (chapters 23-25) and wind tunnels in compressible flow (chapters 26-33). Contributions from a large number of international experts make this publication a highly valuable resource in wind tunnels and fluid dynamics field of research.

How to reference
In order to correctly reference this scholarly work, feel free to copy and paste the following:

Keld Rømer Rasmussen, Jonathan Merrison and Per Nornberg (2011). Wind Tunnels for the Study of Particle Transport, Wind Tunnels and Experimental Fluid Dynamics Research, Prof. Jorge Colman Lerner (Ed.), ISBN: 978-953-307-623-2, InTech, Available from: http://www.intechopen.com/books/wind-tunnels-and-experimental-fluid-dynamics-research/wind-tunnels-for-the-study-of-particle-transport

InTech Europe
University Campus STeP Ri
Slavka Krautzeka 83/A
51000 Rijeka, Croatia
Phone: +385 (51) 770 447
Fax: +385 (51) 686 166
www.intechopen.com

InTech China
Unit 405, Office Block, Hotel Equatorial Shanghai
No.65, Yan An Road (West), Shanghai, 200040, China
中国上海市延安西路65号上海国际贵都大饭店办公楼405单元
Phone: +86-21-62489820
Fax: +86-21-62489821